JOURNAL OF MATERIALS SCIENCE 35 (2000) 437–442

Zr surface diffusion in tetragonal yttria stabilized zirconia

AKASH, M. J. MAYO
Department of Materials Science and Engineering, The Pennsylvania State University, University Park, PA 16802 USA

The value for surface diffusivity of Zr tetragonal ZrO_2–3mol % Y_2O_3 has been calculated from measurements of surface area reduction and pore growth in powder compacts during sintering. The surface diffusivity thereby obtained can be described by $D_{s,Zr^{+4}} = 5.52 \times 10^5 \exp[-531(\text{kJ mol}^{-1})/RT]\ \text{m}^2/\text{s}$, which is in reasonable agreement with values calculated by prior researchers from direct TEM observation of neck growth between touching particles.

1. Introduction

Zirconia has been recognized for its applications in solid oxide fuel cells, [1] thermal barrier coatings, [2] superplasticity, [3] and oxygen sensors and pumps [4]. Knowledge of diffusivities of the constituent ions in ZrO_2 is useful in predicting its performance in these industrial applications. Direct determinations of self-diffusion coefficients of the constituent ions (Zr^{+4}, O^{-2}, and various dopant ions) have been conducted only for a few zirconia-based systems. These are primarily lattice and/or grain boundary diffusion measurements. Specifically, Rhodes and Carter [5] determined cation lattice diffusion coefficients in CaO-ZrO_2 system by tracer techniques. Oishi, Sakka, and Ando determined Zr-Hf lattice interdiffusion coefficients in a 16CaO-84$(Zr + Hf)O_2$ solid solution [6]. In their subsequent work, the same authors calculated the lattice and grain boundary Zr-Hf interdiffusion coefficients in the Y_2O_3-ZrO_2-HfO_2 system [7]. While most studies have been made in cubic zirconia systems, at least one diffusion study has been made to date for zirconium ion (Zr^{+4}) diffusion in a tetragonal zirconia. Sakka *et al.* [8] chose the ZrO_2-CeO_2 system over the ZrO_2-Y_2O_3 system since the narrow single-phase tetragonal region in the latter makes it an inconvenient system for diffusion study. They then described the lattice interdiffusion coefficients by $D_{L,Zr^{+4}} = 3.0\ (10)^3 \exp[-623\ (\text{kJ/mol})/RT]\ \text{cm}^2/\text{s}$ and the grain boundary interdiffusion coefficients by $\delta D_{b,Zr^{+4}} = 0.29\ \exp[-506\ (\text{kJ/mol})/RT]\ \text{cm}^3/\text{s}$. Thus, the lattice and grain boundary diffusivities of Zr^{+4} and O^{-2} ions have been reasonably well documented for cubic and tetragonal zirconia systems. However, no direct surface diffusion study has been carried out for the case of surface diffusion in tetragonal zirconia, especially the ZrO_2-Y_2O_3 solid solution.

An indirect way of measuring self diffusion coefficients is by conducting sintering studies. By this route Kingery and Berg [9] and Kuczynski [10] were able to calculate a self diffusion coefficient of copper which was in reasonable agreement with the existing data. Johnson [11] later postulated a new method to obtain volume, grain boundary, and surface diffusion coefficients from sintering data, even when more than one mechanism was operating simultaneously.

1.1. Surface diffusivity from neck growth studies

Of the different kinds of diffusion, surface diffusion is particularly amenable to measurement via sintering studies, since it is well understood that surface diffusion is the dominant mass transport mechanism during initial stage sintering (neck growth), and under conditions where the sintering temperature is much below the temperature where significant shrinkage commences. Hence, using initial stage neck growth data, surface diffusion data can be calculated with reasonable accuracy. For ceramics, it should be noted that the diffusional transport of matter during densification is controlled by the slowest-moving species; thus in ZrO_2, sintering measurements reflect the movement of the slower Zr^{+4} ions rather than the faster O^{-2} ions.

During initial stage sintering, neck growth between particles (Fig. 1) occurs without any bulk shrinkage of the powder compact [9]. Thermodynamically, there is a maximum in the neck size that can be obtained during this stage which corresponds to a minimum in the surface area of the system [12]. The attainment of a maximum in neck size has been experimentally verified for initial stage sintering in several ceramics [13–15]. The maximum value of neck size can be indirectly calculated from the minimum observed surface area by using the following relation [12]:

$$A = A_{\text{initial}}\left[1 + \frac{c}{4}\left(\frac{x}{R}\right)^2\left(\frac{x}{R} - 1\right)\right], \quad \text{and } x = R\,\text{Sin}\theta, \tag{1}$$

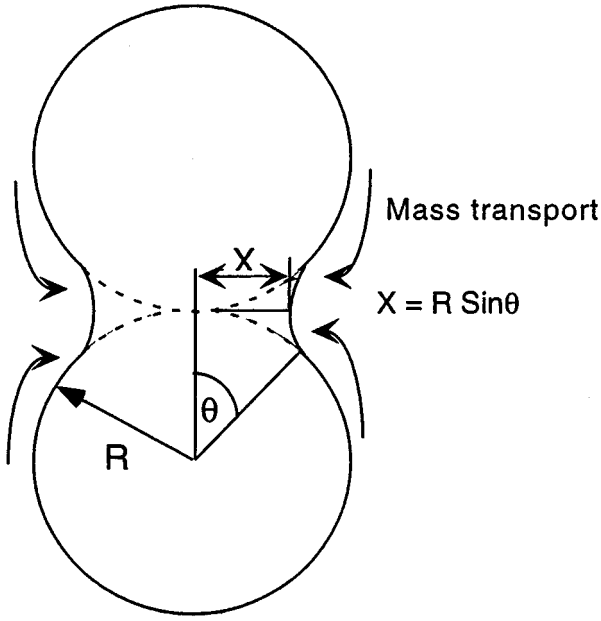

Figure 1 Two sphere model—geometrical calculations (after Kingery and Berg [9]).

where A is the surface area of the system during a certain stage of neck growth, A_{initial} is the initial surface area of the green compact, x is the neck size, R is the particle radius (Fig. 1), and c is the coordination number of particles in the compact. Differentiating with respect to (x/R) gives the minimum possible value of A, which corresponds to the maximum possible value of x/R of 0.5:

$$A_{\text{final}} = A_{\text{initial}}\left[1 - \frac{c}{4} \times 0.125\right] \tag{2}$$

The kinetics of neck growth between two particles in contact can be calculated from Kuczynski's model [10] if D_s is known:

$$\left(\frac{x}{R}\right)^7 = \frac{56 D_s \delta_s \Omega \gamma_{sv}}{kT} \frac{1}{R^4} t. \tag{3}$$

In this equation, x is the neck size, R is the particle radius (Fig. 1), D_s is the surface diffusion coefficient, δ_s is the surface layer thickness (assumed to be 0.3 nm), Ω is the atomic volume, γ_{sv} is the surface energy (assumed to be isotropic), t is the time, and kT have their usual meaning. Thus, when the measured surface area reaches its minimum value, or when $x/R = 0.5$, D_s can be calculated from Equation 3. In practice, the uncertainty in published or assumed values for δ_s and γ_{sv} often prevents an accurate assessment of D_s. In this case Equation 3 provides a measurement of the grouped quantity $(D_s \delta_s \gamma_{sv})$.

1.2. Surface diffusivity from pore shape equilibration studies

A second approach to calculating surface diffusivity is suggested by a recent study [16] which describes the "bumpiness" of pore channel walls as a direct consequence of the fact that the pore walls are originally

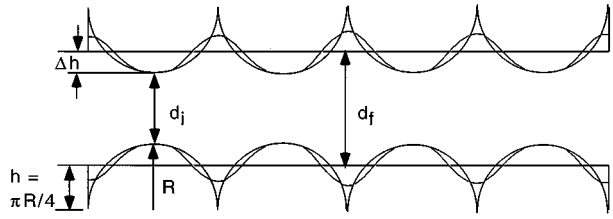

Figure 2 Evolution of pore surface (pore smoothing) along its length, during sintering, stops when the "bumpiness", or the constrictions along the length, disappear, which also marks the end of the pore growth process (figure not to scale).

lined with spherical particles. As sintering proceeds, the surface irregularities in the pore channel are reduced, presumably by a surface diffusion process. The reduction in pore surface area can be observed directly or can be measured as an increase in the (measured) pore size (note that the pore size that is measured by gas adsorption techniques always corresponds to the narrowest constriction of the pore channel). The smoothing process continues until the variation in the pore cross-sections completely evens out (i.e., all the constrictions disappear), which then also marks the end of the apparent pore growth process (Fig. 2). It should be noted that both neck formation between particles (in initial stage sintering) and pore smoothing (in intermediate stage sintering) will lead to an increase of apparent pore size, as measured by the gas adsorption technique, to some equilibrium value. However, in the case of neck formation, the equilibrium pore size persists over a significant period of time, with no change in sample density. In the case of pore smoothing, the equilibrium pore size persists while the sample is densifying considerably.

Since pore smoothing is a surface diffusion driven process, a surface diffusivity value can be extracted from pore geometry equilibration data using a kinetic model for pore smoothing [16]. For this calculation, the following relation is used, as defined in an earlier communication [16]:

$$t^* = \frac{Bt}{R^4} = \frac{D_s \gamma \Omega^{4/3}}{kT \cdot R^4} t, \tag{4}$$

where t^* is the normalized, dimensionless time (note that B/R^4 has the dimension of 1/time), t is the actual sintering time, B is a temperature dependent term, and the remaining terms are the same as in Equation 3. Here, t^* is the time required for completion of the pore smoothing process. As derived in Ref. 16, $t^* = 0.5$ for a pore channel lined with spherical particles; this value holds irrespective of particle size. Thus, any combination of t and T which results in complete pore smoothing (observed in porosimetry as reaching an equilibrium in pore size) allow a value of D_s to be calculated for that temperature using Equation 4.

In the present work, pore smoothing data from the intermediate stage sintering of nanocrystalline zirconia are compared to this model in order to back calculate a surface diffusivity. Thus, in the present work, data from two processes—neck growth and intermediate stage pore smoothing—are used to generate an estimate of surface diffusivity of Zr^{+4} in ZrO_2-3 mol % Y_2O_3.

2. Experimental

2.1. Sample preparation and sintering

Two types of zirconia powders were used. For pore smoothing studies, a nanocrystalline ZrO_2-3 mol% Y_2O_3 powder was used because the absolute time required for pore smoothing scales as particle size to the fourth power [16] and it was desirable to keep the experiment on a reasonable time scale. In neck growth studies, a commercial, submicron powder of the same composition was employed, as it had more reliable initial stage sintering behavior.

2.1.1. Initial stage sintering (neck growth) experiments

Commercial zirconia powders (ZrO_2-3 mol% Y_2O_3) were obtained from the Tosoh company (Tokyo, Japan). The commercial Tosoh powders consisted of aggregate particles, most of which were between 0.08 to 0.40 μm, with an average size around 0.30 μm, as measured from transmission electron microscopy (TEM) [18]. These aggregate particles were comprised of individual crystallites, which were strongly bonded to each other, with almost no porosity between them. X-ray line broadening (XRLB) results showed the average size of the crystallites to be 35 nm. The Tosoh samples were uniaxially dry pressed at 1.8 GPa. The green samples were sintered in air at 870 °C (heating rate: 5 °C/min.) for times ranging from 0 to 25 h.

2.1.2. Intermediate stage sintering (pore smoothing) experiments

The second set of powder called "nanocrystalline", was prepared by chemical coprecipitation [17]. Prior TEM studies have shown this product to consist of weakly agglomerated, well-faceted, and almost equiaxed primary crystallites [18]. A value of 13 nm was obtained for the crystallite size, as calculated from gas adsorption analysis, for the powders used in this study. XRLB measurements (Scherrer method) gave a value of 15 nm for the primary particle size of the powders and green compacts, which was consistent with the BET results. The powders were then consolidated by centrifugation.

Approximately 4 g of powder was suspended in 350 ml of ethanol after pH adjustment by nitric acid additions to a pH of 0.5–0.6. The suspension was then put in an ultrasonic bath for 10 min. Next, the suspension was separated into ten 50 ml centrifuge tubes, each containing 35 ml of the suspension, and centrifuged in a Beckman model TS-6 centrifuge at 5800 rpm (3900 RCF (g) or 0.1 MPa) for 20 min. The supernate was decanted and the consolidated samples were refrigerator dried for 4–5 days in an ethanol saturated ambient. The nanocrystalline samples were sintered in air at temperatures ranging from 793 to 1050 °C for times up to 5 h. A heating rate of 2 °C/min was used.

Samples that were sintered for 0 and 5 min were immediately taken out from the bottom loading furnace (Carbolite 1700) upon completion of their sintering schedule, and were air quenched to room temperature. All other samples were furnace cooled to room temperature.

2.2. Characterization

2.2.1. Density measurements

The Archimedes technique was used to measure the density of all green and sintered samples. The Tosoh samples were heated at 600 °C (3 °C/min) for 3 h to burn off all the binder before conducting any density or pore size measurements. In order to impart coherency and strength to the nanocrystalline (green) samples when placed in water, the samples were heated (2 °C/min) at 500 °C for 2 h. TMA (Thermo-Mechanical Analysis) results confirmed that no shrinkage occurred in the nanocrystalline samples until well over 500 °C. Although all the nanocrystalline green and Tosoh samples had undergone some heat treatment prior to sintering, they will still be referred to as green (or initial) samples in this study. All the nanocrystalline samples had an initial (green) density of 49%, while the Tosoh (green) samples were measured to be 62% dense.

2.2.2. Grain size measurements

Grain size was determined for the nanocrystalline samples only, as the temperatures to which the commercial powder was exposed were too low for detectable grain growth. Grain size was measured by XRLB. The grain diameter (also known as the crystallite size or the domain size) was obtained using the Scherrer equation [19]:

$$d = \frac{0.94\lambda}{\beta_{hkl}\mathrm{Cos}\theta} \tag{5}$$

where, λ is the X-ray wavelength (in Å), θ is the Bragg angle of the (hkl) reflection, and β_{hkl} is the full width at half maximum (FWHM) of the (hkl) reflection profile with instrumental broadening removed. The instrumental broadening was found from the reflection given by a single crystal quartz sample. The instrumental broadening thus calculated was subtracted from that obtained for the sample, to get the peak broadening or the FWHM due only to the sample. The X-ray diffraction data was collected in the 2θ range of 27–35°, corresponding to the [1 1 1] reflection of tetragonal zirconia. To ensure the accuracy of the peak shape, step scans were performed at a sufficiently slow scanning rate of 0.1°/min, so that no smoothing of the peaks was necessary. Background intensity was stripped by the least squares method. All the samples were polished to a 0.25 mm finish prior to grain size measurements.

The results obtained by XRLB were compared with those obtained from scanning electron microscopy. Reasonable agreement was obtained between the two.

2.2.3. Pore size distribution measurement

A (nitrogen) gas adsorption technique was used to determine the pore size distribution in the green and in

the sintered samples. Apparent pore size was calculated from the Kelvin equation [20]:

$$r_c = \frac{-4.15}{\log\left(\frac{P}{P_o}\right)}(\text{Å}) \quad (6)$$

where P/P_o is the relative pressure of gas at which the core of the pore of radius r_c becomes filled, and P_o is the equilibrium pressure of gas over a flat surface. For a pore channel of uneven cross-section along its length, the whole pore channel is filled only when the relative pressure reaches the value corresponding to the maximum existing cross-section of the pore channel, while it is emptied only when the relative pressure decreases to a value corresponding to the narrowest pore cross–section [19]. A Micromeritics ASAP 2010 was used for all gas adsorption measurements.

3. Results and discussion

3.1. Calculation of D_s from neck growth observations (initial stage sintering)

Data from initial stage sintering experiments on Tosoh zirconia (Table I and Fig. 3) indicates that the total surface area reaches a minimum of 1/1.28 of its initial value after sintering for around 15–17 h at 870 °C. Thus, Equation 2 predicts that for a 62% green density sample (the coordination number, c, is 7 [16]) equilibrium should be reached at $A_{final} = A_{initial}/1.28 = 0.785\ A_{initial}$. The fact that neck growth equilibrium occurs at exactly the predicted theoretical value suggests the corresponding kinetic equation for neck growth (Equation 3) should apply without ambiguity. To obtain D_s from Equation 3, the appropriate values of all the variables are substituted into that equation ($R = 0.15\ \mu$m; $T = 870$ °; $t = 16$ h; $\delta_s = 0.3$ nm; $\Omega = 3.35 \times 10^{-29}$ m^3; $k = 1.38 \times 10^{-23}$ J/K; and $\gamma_{sv} = 0.3$ J/m^2), yielding a D_s value of around 6.0×10^{-18} m^2/s at 870 °C. This is in good agreement with the values of surface diffusion calculated by Rankin and Sheldon [14] on pure, unstabilized zirconia from their TEM observations at 890 °C. These researchers studied the neck growth behavior of single crystal particles of pure ZrO_2 using in situ transmission electron microscopy. They also applied Kuczynski's [10] relationship for neck growth to their observations and were able to obtain a value of 10^{-16}–10^{-17} m^2/s for surface diffusion at 890 °C. A separate calculation of D_s using high resolution still images of individual atom movements (random-walk of single atoms) on the edges of sintering ZrO_2 particles surface gave values of D_s in the range of 2×10^{-17} to 2×10^{-18} m^2/s [14]. Rankin and Sheldon [14] attributed the order of magnitude difference in the two predictions to the fact that in reality, atom movement was often taking place by motion of "clusters" of atoms (10–100 atoms) rather than "individual" atoms.

TABLE I Initial stage sintering results for Tosoh (TZ-3Y) samples at 870 °C

Time (h)	Initial density (% theo.)	Sintered density (% theo.)	Ratio of final to initial surface area (A_f/A_i)
10	63.7	64.4	0.846
15	64.4	68.7	0.773
17.5	64.6	68.1	0.790
20	64.7	65.8	0.777
22.5	64.0	69.0	0.786
25	65.1	65.2	0.786
30	63.9	65.2	0.759

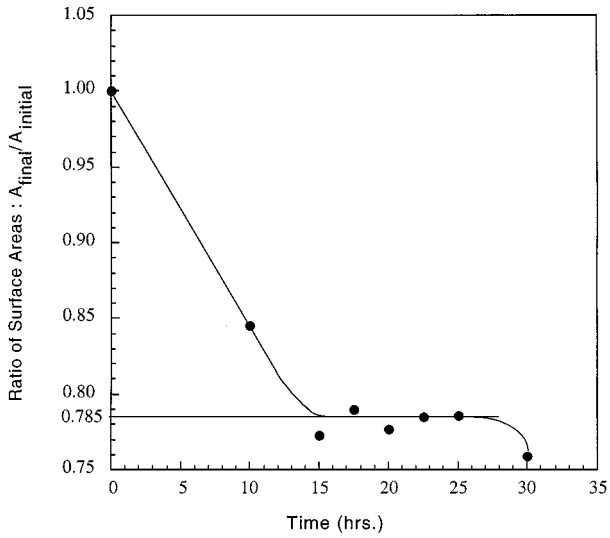

Figure 3 Initial stage sintering of (commercial) Tosoh zirconia at 870 °C.

3.2. Calculation of D_s from pore smoothing observations (intermediate stage sintering)

From the pore smoothing model, the value of t^* at which the pore geometry equilibration process is complete is 0.5 [16]. It should be noted that t^* is a dimensionless parameter, i.e., different combinations of T and t in the above equation can give the same value of t^*. Results for nanocrystalline ZrO_2-3 mol % Y_2O_3 show that it requires five hours at 900 °C for the completion of the pore geometry equilibration process or 30 min at 1000 °C or 5 min at 1050 °C (Fig. 4 and Table II). Because diffusion data are available for several temperatures (using Equation 4; see Table II), it is possible to calculate both a pre-exponential factor and an activation energy for D_s, as shown in Fig. 5. The resulting expression for D_s is $D_s = 5.52\ (10)^5 \exp[-531\ (\text{kJ/mol})/RT]$ m^2/s. The values of R ($= G/2$, where G is the grain size), T, and t used for these calculations are listed in

TABLE II Calculation of D_s using the minimum time required at different temperatures for completion of the pore smoothing (pore geometry equilibration) process (Equation 4)

Temperature (°C)	Minimum time	Grain size (G) at $t = 0$ min (nm)	Final pore size (Å)	D_s (calculated) (m^2/s)
900	5 h.	20	197	$1.38859\ (10)^{-18}$
1000	30 min	28	197	$5.7892\ (10)^{-17}$
1050	5 min	34	190	$7.8484\ (10)^{-16}$

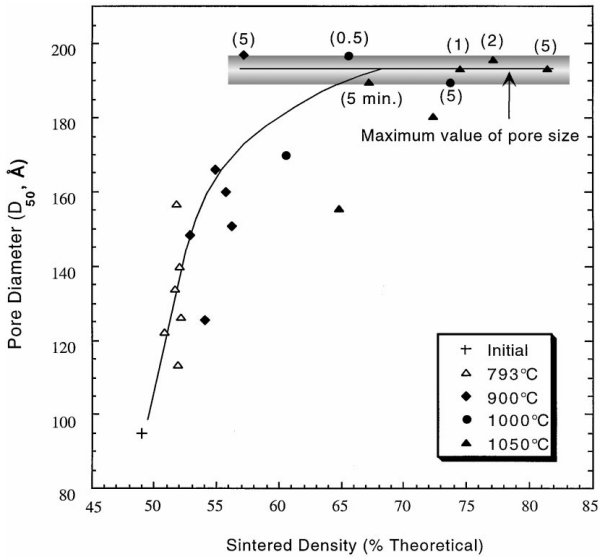

Figure 4 Pore size-density trajectory for nanocrystalline samples show that the pore size reaches a maximum value independent of the sintered density. Time, in hours, is shown in parentheses.

Table II (all the other constants are identical to those in Equation 3).

The diffusivity at 900 °C, obtained from the above calculations [1.4×10^{-18} m^2/s, Table II], are in reasonable agreement with that calculated from neck growth data, in the previous section, at 870 °C [6×10^{-18} m^2/s]. Further, the calculated values of diffusion coefficient at 900 °C (Table II), using the pore smoothing data, are in reasonable agreement with the values calculated by Rankin and Sheldon [14] from the TEM experiments at 890 °C ($D_s = 1.38 \times 10^{-18}$ m^2/s vs. 2×10^{-18} m^2/s $< D_s < 10^{-17}$ m^2/s). In addition, an interesting comparison can be made between surface diffusion values calculated in Table II and the grain boundary diffusion values reported in the literature for tetragonal zirconia (stabilized with ceria). Sakka *et al*. [8] reported a value of 967 m^2/s (assuming the same $\delta = 0.3$ nm) for $D_{o,gb}$ and 506 kJ/mol for Q_{gb}. In the present study, the Q for surface diffusion is found to be 531 kJ/mol (Fig. 2)—close to Sakka *et al*. Q_{gb} [8]—while the pre-exponential factor is orders of magnitude larger (5.5×10^5 vs. 967 m^2/s). These results suggest that the local atomic environment in which atoms are moving is very similar for both free surface and grain boundaries (i.e., their "successful" jump frequency is similar), but that the number of such sites available is vastly increased in the case of the free surface.

4. Conclusions

The surface diffusion values for Zr^{+4} ions in ZrO_2-3 mol % Y_2O_3 have been calculated by comparing neck

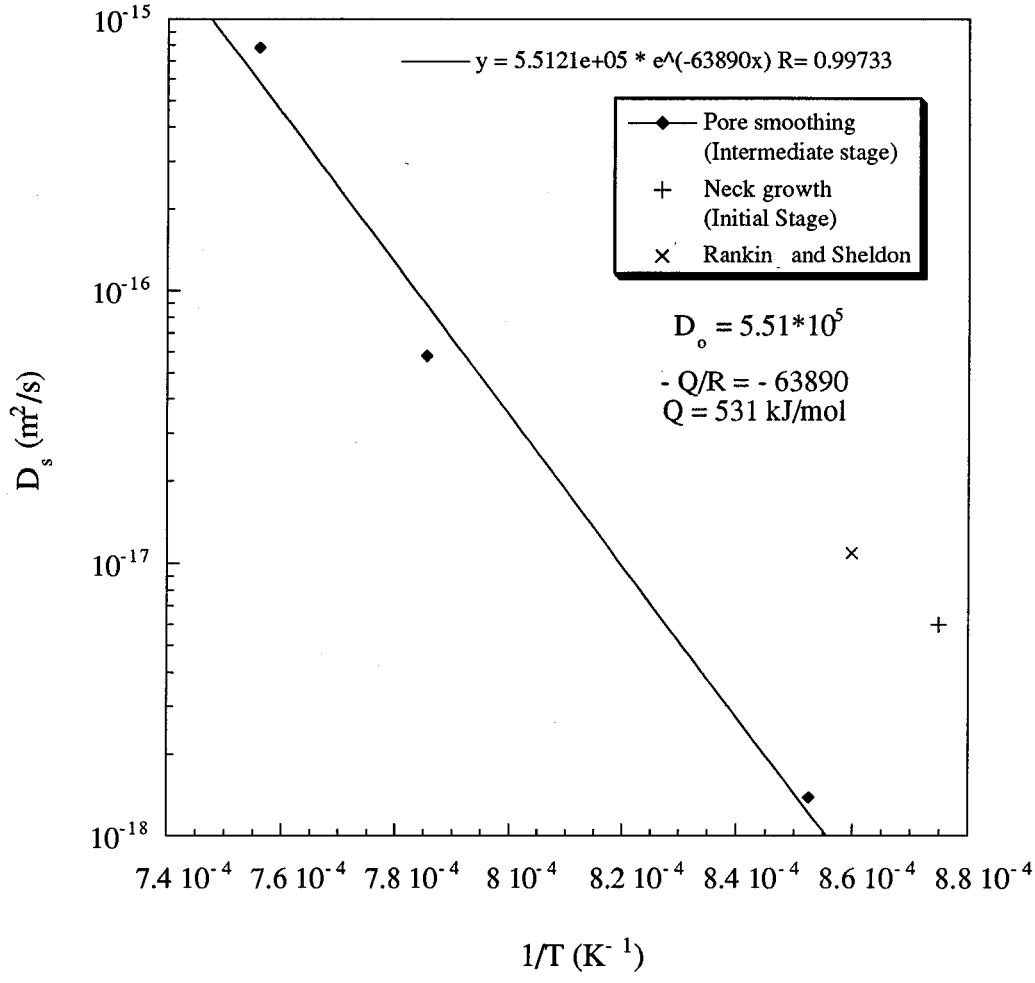

Figure 5 Plot of surface diffusivity values versus reciprocal of temperature for ZrO_2–3 mol % Y_2O_3 gives $D_s = 5.51 \times 10^5 \exp[-531/RT$ (kJ/mol)]. Best fit line for data taken from pore smoothing experiments, though data from neck growth experiments are also shown.

growth and pore smoothing data with available models. Both methods give surface diffusivity values which are in reasonable agreement with each other and with values existing in literature. An Arrhenius relation for surface diffusivity of zirconium ions in tetragonal ZrO_2-3 mol % Y_2O_3 is obtained:

$$D_s = 5.52 \times 10^5 \exp\left(-\frac{531}{RT}\frac{\text{kJ}}{\text{mol}}\right)\text{m}^2/\text{s}$$

Acknowledgement

The authors gratefully acknowledge the support of the Office of Naval Research, contract #N00014-95-1-0574, in funding this work.

References

1. N. Q. MINH, *J. Amer. Ceram. Soc.* **76** (1993) 563.
2. R. A. MILLER, *Surf. and Coating Tech.* **30** (1987) 1.
3. F. WAKAI, S. SAKAGUCHI and Y. MATSUNO, *Adv. Ceram. Mater.* **1** (1986) 259.
4. E. SUBBARAO, in "Science and Technology of Zirconia III," edited by S. Somiya, N. Yamamoto and H. Hanagida (The American Ceramic Society, Westerville OH, 1988) p. 731.
5. W. H. RHODES and R. E. CARTER, *J. Amer. Ceram. Soc.* **49** (1966) 244.
6. Y. OISHI, Y. SAKKA and K. ANDO, *J. Nucl. Mater.* **96** (1981) 23.
7. *Idem., J. Mater. Sci.* **17** (1982) 3101.
8. Y. SAKKA, Y. OISHI, K. ANDO and S. MORITA, *J. Amer. Ceram. Soc.* **74** (1991) 2610.
9. W. D. KINGERY and M. BERG, *J. Appl. Phys.* **26** (1955) 1205.
10. G. C. KUCZYNSKI, *Trans. AIME* **185** (1949) 169.
11. D. L. JOHNSON, *J. Appl. Phys.* **40** (1969) 192.
12. S. PROCHAZKA and R. L. COBLE, *Phys. of Sintering* **2** (1970) 1.
13. E. B. SLAMOVICH and F. F. LANGE, *J. Amer. Ceram. Soc.* **73** (1990) 3368.
14. J. RANKIN and B. W. SHELDON, *Mater. Sci. & Eng.* **A204** (1995) 48.
15. AKASH and M. J. MAYO, *J. Amer. Ceram. Soc*. Submitted (1998).
16. AKASH and M. J. MAYO, *ibid*. Submitted (1998).
17. M.ÇIFTÇIOGLU and M. J. MAYO, in "Superplasticity in Metals, Ceramics and Intermetallics," edited by M. J. Mayo, M. Kobayashi and J. Wadsworth (MRS, Pittsburgh, 1990) p. 77.
18. D-J. CHEN, M. S. Metals Sci. and Eng., The Pennsylvania State University, University Park 1994.
19. H. P. KLUG and L. E. ALEXANDER, "X-Ray Diffraction Procedures for Polycrystalline and Amorphous Materials," (Wiley, New York, 1974).
20. J. H. DE BOER, in "The Structure and Properties of Porous Materials," edited by D. H. Everett and F. S. Stone (Academic Press, New York, 1958) p. 68.

Received 18 February 1998
and accepted 1 April 1999